ADVANCES IN ATMOSPHERIC SCIENCES, VOL. 33, MARCH 2016, 365–376

Climatology of Lightning Activity in South China and Its Relationships to Precipitation and Convective Available Potential Energy

Dong ZHENG*[1,2], Yijun ZHANG[1,2], Qing MENG[1,2], Luwen CHEN[3], and Jianru DAN[4]

[1]*State Key Laboratory of Severe Weather, Chinese Academy of Meteorological Sciences, Beijing* 100081

[2]*Laboratory of Lightning Physics and Protection Engineering, Chinese Academy of Meteorological Sciences, Beijing* 100081

[3]*Lightning Protection Center of Guangdong Province, Guangzhou* 510080

[4]*Conghua Meteorological Bureau, Guangzhou* 510925

(Received 15 May 2015; revised 16 September 2015; accepted 18 September 2015)

ABSTRACT

This study examined lightning activity and its relationship to precipitation and convective available potential energy (CAPE) in South China during 2001–12, based on data from the Guangdong Lightning Location System, the Tropical Rainfall Measuring Mission satellite, and the ERA-Interim dataset. Two areas of high lightning density are identified: one over the Pearl River Delta, and the other to the north of Leizhou Peninsula. Large peak-current cloud-to-ground (LPCCG) lightning (>75 kA) shows weaker land–offshore contrasts than total CG lightning, in which negative cloud-to-ground (NCG) lightning occurs more prominently than positive cloud-to-ground (PCG) lightning on land. While the frequency of total CG lightning shows a main peak in June and a second peak in August, the LPCCG lightning over land shows only a single peak in June. The ratio of positive LPCCG to total lightning is significantly greater during February–April than during other times of the year. Diurnally, CG lightning over land shows only one peak in the afternoon, whereas CG lightning offshore shows morning and afternoon peaks. The rain yield per flash is on the order of 10^7–10^8 kg per flash across the analysis region, and its spatial distribution is opposite to that of lightning density. Our data show that lightning activity over land is more sensitive than that over offshore waters to CAPE. The relationships between lightning activity and both precipitation and CAPE are associated with convection activity in the analysis region.

Key words: climate characteristics, lightning, precipitation, CAPE, large peak current, land–offshore contrast

Citation: Zheng, D., Y. J. Zhang, Q. Meng, L. W. Chen, and J. R. Dan, 2016: Climatology of lightning activity in South China and its relationship to precipitation and convective available potential energy. *Adv. Atmos. Sci.*, **33**(3), 365–376, doi: 10.1007/s00376-015-5124-5.

1. Introduction

Improvements in lightning detection techniques in recent decades have contributed greatly to our understanding of lightning activities and related phenomena (e.g., Cummins et al., 1998; Shindo and Yokoyama, 1998; Boccippio and Christian, 1999; Pinto et al., 1999a, 1999b; Orville and Huffines, 2001; Orville et al., 2002; Ma et al., 2005a; Betz et al., 2009; Chen et al., 2012). Climatological aspects of lightning activity can represent spatiotemporal patterns of deep convective activity, which can also act as effective indicators of climate change (e.g., Reeve and Toumi, 1999; Ma et al., 2005b; Zipser et al., 2006). Hence, lightning activity has been widely studied in different regions for a variety of purposes (e.g., Hidayat and Ishii, 1998; Orville and Huffines, 2001; Altaratz et al., 2003; Christian et al., 2003; Qie et al., 2003a, 2003b; Kandalgaonka et al., 2005; Ma et al., 2005a; Kuleshov et al., 2006; Rudlosky and Fuelberg, 2010). Research has demonstrated the apparent dependence of lightning activity on climatic and geographic conditions in different regions. In addition, the relationships between lightning activity and meteorological phenomena have been a focus of research for many years (e.g., Price, 1993; Baker et al., 1995; Petersen and Rutledge, 1998; Sherwood et al., 2006; Zheng et al., 2010; Romps et al., 2014), and have contributed greatly to our understanding of the atmospheric thermodynamic mechanisms and functions that drive climate models.

In this study, special attention was paid to lightning activity in South China and its relationship to precipitation and convective available potential energy (CAPE), for the following reasons: (1) South China, a densely populated and economically developed area, features the highest frequency of lightning activity, as well as the greatest number of lightning casualties and damage in all of China, as inferred from both global and Chinese lightning distribution maps (e.g., Christian et al., 2003; Ma et al., 2005a) and lightning disaster

* Corresponding author: Dong ZHENG
Email: zhd@cams.cma.gov.cn

analyses (Zhang et al., 2011), respectively. Although some previous studies have explored the climatic characteristics of convective activity and precipitation in South China or its adjacent areas during some seasons (e.g., Yuan and Qie, 2008, Xu et al., 2009; Zheng and Cheng, 2011; Luo et al., 2013; Wu et al., 2013; Xu, 2013), lightning activity as a possible proxy for strong convection (Zipser et al., 2006) has seldom been investigated in detail or as the main object of analysis. The expectation, therefore, was that this study will contribute to an improved understanding of deep convective activity and lightning discharges in South China, and provide a basic reference for lightning risk assessment and lightning protection guidelines. (2) As a relatively new type of data in the observation of convective weather in China, cloud-to-ground (CG) lightning data observed by the Guangdong Lightning Location System (GDLLS), constructed by State Grid Electric Power Research Institute starting in 1996, provide probably the longest continuous climatology–lightning dataset (both spatially and temporally) in China, thus facilitating a reliable analysis of climate–lightning relationships. Although some previous studies have reported the characteristics of local lightning activity in Guangdong (e.g., Zhang et al., 2000; Yi et al., 2006), their lightning data were limited in time span and spatial range.

In addition to the above considerations, we were further concerned with occurrences of large peak-current CG (LPCCG) lightning (peak currents of >75 kA) and the possible contrast between CG lightning activity over land and over offshore waters. LPCCG lightning, because of its destructiveness and association with sprites and elves in the stratosphere and mesosphere, has been of particular concern in the research community (e.g., Lyons et al., 1998; Kochtubajda et al., 2006; Pinto et al., 2009). In addition, the land–offshore lightning comparison provides another perspective from which to understand the impact of underlying surfaces on convective activity and lightning discharge.

2. Study area and data

2.1. *Study area*

The study area, delineated by the red line in Fig. 1, includes the land part of Guangdong and a portion of offshore waters in the South China Sea. The offshore boundary of the study region is $\sim$100 km from the coastline, to ensure reliable detection of lightning activity by the GDLLS over offshore waters. The total area of $\sim$244 000 km^2 included $\sim$180 000 km^2 of land and $\sim$64 000 km^2 of offshore waters.

Two rainy seasons occur in the study area: a pre-summer rainy season and a post-flooding rainy season (Ding and Wang, 2008). The pre-summer rainy season generally occurs from April to June, and is controlled by midlatitude weather systems. The monsoon, which typically occurs in the pre-summer rainy season, has been widely studied (e.g., Yuan and Qie, 2008; Xu et al., 2009; Zheng and Cheng, 2011; Luo et al., 2013; Xu, 2013). During the active monsoon period (roughly from mid-May to mid-June), precipitation over

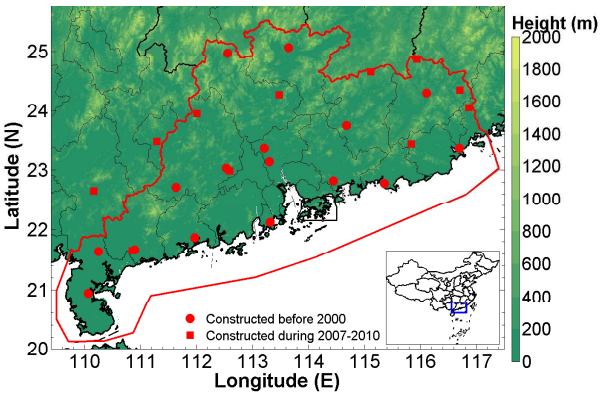

Fig. 1. Terrain map of the study area in South China. The study region is delineated by the red line; red dots show the positions of GDLLS sensors. The insert map (lower right) shows the location of the study area within China.

South China (an area larger than Guangdong) is characterized by extensive rainbands with a near east–west orientation. The mesoscale convective system, driven typically by dynamic processes such as surface fronts and low-level shear lines, is the dominant rainfall producer, accounting for $\sim$90% of the total near-surface rainfall. Some parameters associated with storm structures suggest that convection intensifies progressively from the pre-monsoon to the monsoon to the post-monsoon periods, which is largely in agreement with variations in the CAPE and total precipitable water. The second rainy season generally occurs from July to September, when large-scale precipitation is usually produced by tropical cyclones and other tropical weather systems. In addition, the convection driven by thermodynamic processes is remarkably strong.

2.2. *Data and their processing*

Three types of data were used in this study: CG lightning data from the GDLLS; total lightning (intra-cloud lightning and CG lightning) and precipitation data from the Tropical Rainfall Measuring Mission (TRMM); and CAPE data from the ERA-Interim dataset provided by the European Centre for Medium-Range Weather Forecasts (ECMWF).

Construction of the GDLLS started in 1996, and by 2000 the GDLLS consisted of a network of 16 time-of-arrival/magnetic direction sensors (see Fig. 1). During 2007–10, the GDLLS was upgraded and the number of sensors was increased to 27, including two new sensors in Guangxi Province to the west of Guangdong (see Fig. 1). The data used in this study cover the period 2001–12.

Theoretically, an increase in the number of sensors in the network should improve the detection efficiency and precision of lightning discharges. For example, Chen et al. (2002) reported that in 1999, when 14 sensors were present in the network, the CG flash detection efficiency of the GDLLS was 86%, and the median error of the location accuracy was 1.3 km. However, based on artificially triggered lightning and optical lightning records during 2007–11, Chen et al. (2012) determined that the CG flash detection efficiency had

increased to ∼94%, the median location error had decreased to ∼489 m, and the median percentage error of the peak current was ∼19.1%. Thus, upgrades to the GDLLS increased the accuracy of analyses, based on the GDLSS data. Moreover, variations in the detection efficiency and precision did not adversely affect the conclusions of this study, as: (1) according to the above two studies (Chen et al., 2002, 2012), the detection efficiencies of the network of CG flashes during different periods were all relatively high, and the improvements were relatively moderate; and (2) system updates did not substantively impact comparative analyses of the spatial distribution or temporal distribution (in months and hours) of lightning activity.

On the other hand, changes in the nature of the data might be problematic and deserve extra investigation. In Table 1, we list some parameters associated with the raw return stroke (RS) data (a CG lightning flash consists of one or more return strokes, which are the objects of a CG lightning location system) within the analysis region during the periods 2001–06 (before the update), 2007–10 (during the update), and 2011–12 (after the update). After the GDLLS update, the number of sensors involved in the location of RSs in different peak-current intervals increased significantly, while the ratios of RSs within different peak-current intervals to the total RS number and the mean RS current remained steady, with only small variations. Therefore, the upgrade to the GDLLS apparently did not impact the nature of the observational data, and thus the data are deemed reliable.

The criterion used for grouping the RSs with a lightning flash is that adjacently located return strokes for a single flash should occur within a 0.5-s interval and a 10-km distance. The average position of the RSs recorded by the largest number of sensors was specified as the flash position, and the maximum peak current among the RSs was considered to be the flash current. We used the criterion for acceptable flash current data that the flash current must have been located by at least three sensors, thus ensuring the reliability of the data. In previous studies (e.g., Cummins et al., 1998), positive CG (PCG) lightning flashes with currents of $<$10 kA were removed from the data as they might be a misinterpretation of cloud lightning. Furthermore, following the subjective definition of Lyons et al. (1998) and Pinto et al. (2009) of LPCCG lightning, the CG lightning with an absolute peak current of $>$75 kA was selected as LPCCG lightning. The ratio of LPCCG lightning to total CG lightning was 5.20%; in comparison, a ratio of 2.46% has been reported over the contiguous United States during the summer months (Lyons et al., 1998), and a ratio of 3% has been reported over southeastern Brazil (Pinto et al., 2009).

Table 1. Parameters associated with the return stroke (RS) data in the analysis region (data from the GDLLS).

Parameters		2001–06	2007–10	2011–12
Number of sensors involved in the location	Total RSs	5.3	6.0	8.5
	$RS_{<50kA}$	5.0	5.3	7.1
	$RS_{>75kA}$	7.4	11.1	22.3
Percentage (%)	$RS_{<50kA}$	90.5%	87.1%	89.9%
	$RS_{>75kA}$	3.5%	4.5%	3.7%
Mean current (kA)	Total RSs	27.7	29.8	26.1
	$RS_{<50kA}$	21.5	22.2	20.1
	$RS_{>75kA}$	86.8	81.0	80.0

High Resolution Full Climatology TRMM/Lightning Imaging Sensor (LIS) 0.5° data were used to determine the total lightning activity in the study region. Specific features of the data have been previously described by Daniel et al. (2014). The TRMM 3B43 dataset (including the TRMM and Other Data Precipitation Product) was used to determine the monthly precipitation at a resolution of 0.25°. The CAPE data were extracted from the monthly means of the meteorological reanalysis data of the ERA-Interim data at a resolution of 0.75°.

3. Spatiotemporal characteristics of lightning activity

3.1. *Spatial distribution*

Figure 2 shows the lightning density in the study area counted in the grids of $0.1^\circ \times 0.1^\circ$. Two regions of high lightning density (of both total lightning and total CG lightning) are evident. One region is centered on Guangzhou City (23°N, 113.5°E) near the Pearl River Delta (PRD), where the total lightning density is $>$32 flashes km^{-2} yr^{-1} and the total CG lightning density is $>$15 flashes km^{-2} yr^{-1}. The second region is located to the north of Leizhou Peninsula (21.75°N, 110.5°E), where the total lightning density is $>$26 flashes km^{-2} yr^{-1} and the total CG lightning density is $>$12 flashes km^{-2} yr^{-1}. In the study area, the density of total CG lightning is comparable to that in Florida, United States (e.g., Orville and Huffines, 2001).

Two possible reasons for the strong lightning activity in the two regions were identified. The first is associated with the thermal and aerosol characteristics of Guangzhou City, which may result in high lightning densities relative to the surrounding area, as also reported for other large cities such as Houston (Orville et al., 2001), Seoul (Kar et al., 2009), and Paris (Coquillat et al., 2013). It is thought that the urban heat island effect favors convection over cities, while high concentrations of cloud condensation nuclei (e.g., aerosol) result in larger numbers of small cloud droplets. Under these conditions, the droplets can be more effectively carried above the freezing level to enhance riming and then charging processes (e.g., Williams et al., 2002, 2004). In support of this scenario, Wang et al. (2011) simulated variations in the lightning potential index under pollution conditions in the PRD area, and documented a 50% enhancement.

The second possible cause of strong lightning activity in the two regions is associated with terrain and local circulation patterns. A comparison of Figs. 1 and 2 shows that the two regions with frequent lightning flashes are both bordered on one side by mountains, and both exposed to the ocean on another side in the topography. According to ERA-Interim

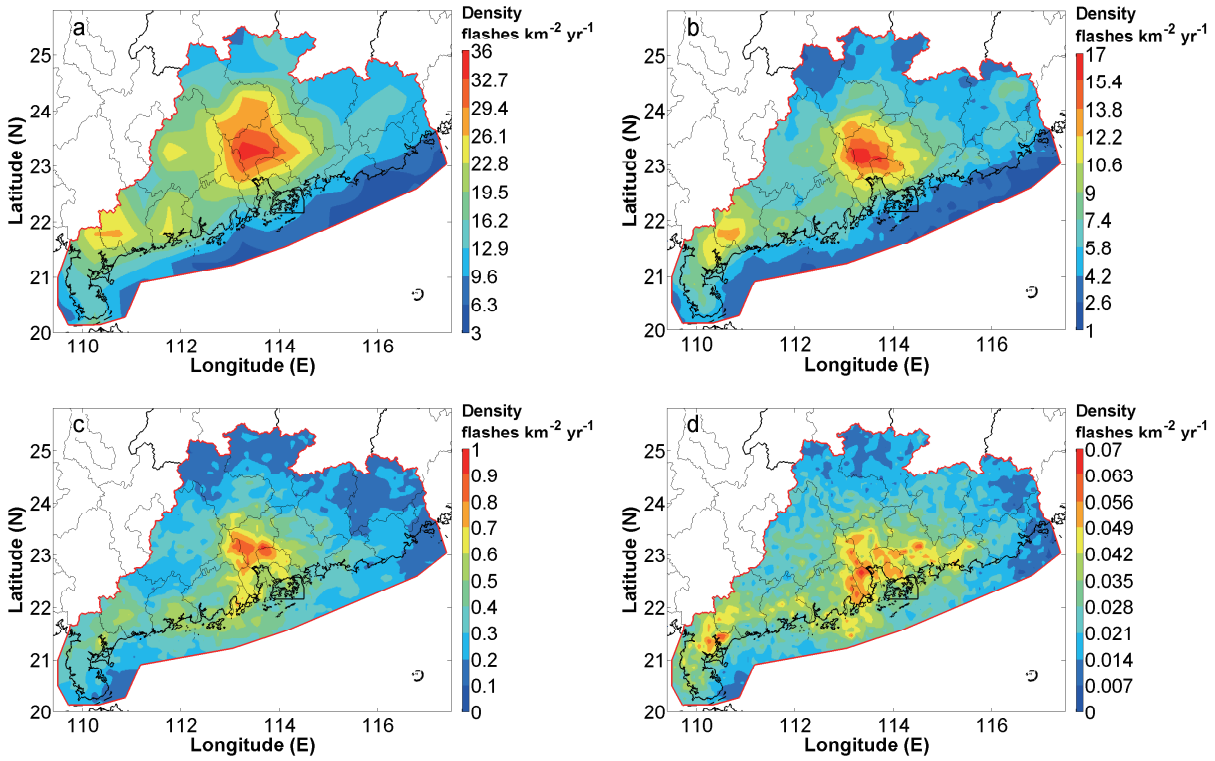

Fig. 2. Densities of (a) total lightning, (b) total CG lightning, (c) LPCCG lightning, and (d) positive LPCCG lightning.

wind-field data at 850 hPa, the dominant airflow during the rainy season (especially during April–August) is from the ocean, and hence carries abundant water vapor. Thus, the terrain surrounding the two regions favors the convergence of airflow, which may support enhanced convective activity in these regions. The combined effects of terrain and local circulation have also been discussed by Luo et al. (2013) and Xu et al. (2009) in their studies on convection and precipitation in the region.

Near the coastline, the lightning density decreases sharply from land to offshore areas. This same phenomenon was also reported by Tapia et al. (1998) on the east coast of Florida, and by Steiger and Orville (2003) on the Gulf Coast. Changes in thermal properties are expected to be abrupt along any coastline (Williams et al., 2004), and thus may be responsible for the observed lightning behavior. The PCG lightning generally has a spatial distribution similar to that of total CG lightning (data not shown), except that the highest density of PCG lightning is centered slightly closer to the coastline than in the case of CG lightning.

The land–ocean contrast in lightning frequency follows differences in convection between land and ocean. Studies have shown that convection over land is more intense than over the ocean (e.g., Zipser, 1994; Zipser et al., 2006; Xu et al., 2009; Xu and Zipser, 2012; Wu et al., 2013), a pattern that has been explained by two proposed mechanisms. According to the first, the response of the land to solar radiation is stronger than that of the ocean, thus promoting stronger and/or broader updrafts over land than over the ocean. According to the second, the concentration of cloud condensation nuclei over land is greater than over ocean. The first mechanism (the thermal hypothesis) has garnered more support than the second mechanism (the aerosol hypothesis) (Williams et al., 2002, 2004; Williams and Stanfill, 2002; Kumar and Kamra, 2010).

Figures 2c and d display the density distributions of LPCCG and positive LPCCG lightning, respectively. A comparison of Figs. 2a and c shows that the density of LPCCG lightning is higher over the region close to the coastline. The densities of LPCCG and negative LPCCG lightning flashes are apparently higher over the PRD. However, for the positive LPCCG lightning, two high-concentration regions, one around the mouth of the Pearl River and the other to the north of the Leizhou Peninsula, are connected by a belt of scattered high-density lightning locations. Differences between positive and negative LPCCG lightning densities have also been reported by Lyons et al. (1998) and Pinto et al. (2009).

Table 2 lists the average lightning density over land and offshore regions, including the ratios of the average density over land to that over water. The densities of total lightning and total CG lightning over land are ∼1.8 times those over offshore waters; this ratio is much smaller than the value of ∼10 obtained from global-scale land and ocean lightning data (e.g., Christian et al., 2003; Pan et al., 2013) and the value of ∼13 that was calculated from CG lightning density over Java Island (3.2 flashes km^{-2} yr^{-1}) and over the sea ∼100 km south of Java Island (0.24 flashes km^{-2} yr^{-1}) (as reported by Hidayat and Ishii, 1998).

The statistics in Table 2 further reveal that the differences between land and offshore waters for LPCCG light-

Table 2. Average lightning density statistics for several regions (rounded to two significant digits).

Types of lightning	Whole region (flashes km^{-2} yr^{-1})	Land (flashes km^{-2} yr^{-1})	Offshore waters (flashes km^{-2} yr^{-1})	D_{land}/D_{water}
Total	15.90	18.05	9.90	1.82
CG	6.38	7.24	4.00	1.81
PCG	0.50	0.55	0.37	1.50
NCG	5.88	6.69	3.64	1.84
LPCCG	0.33	0.33	0.33	1.01
+LPCCG	0.027	0.028	0.026	1.08
−LPCCG	0.31	0.31	0.30	1.00

D_{land}, lightning density over land; D_{water}, lightning density over offshore waters.

ning are small, with the land/offshore ratio for LPCCG lightning being close to 1 in the analysis region. On the other hand, the land/offshore ratio for negative cloud-to-ground (NCG) lightning is higher than that for PCG lightning, which indicates a more prominent preference of NCG lightning for land as compared with PCG lightning. However, this situation changes when LPCCG lightning is considered, as the land/offshore ratios for positive LPCCG and negative LPCCG are similar to each other.

3.2. *Temporal variation*

3.2.1. *Monthly distribution*

Figures 3a and b show that most of the CG lightning in the study area occurs during April–September, coinciding with the rainy season (Ding and Wang, 2008). Regardless of the underlying surface, total CG lightning shows two peaks, one in June and one in August. The June peak is stronger, especially over offshore waters. Interestingly, when the LPCCG lightning and positive lightning (including positive LPCCG lightning) are considered, only one peak is evident over land (in June), while two peaks occur over water (in June and August, similar to those of total CG lightning).

Monthly variations in lightning activity are closely related to patterns of convective activity. Zheng and Cheng (2011) found that in South China the frequency of convective activity in June is greater than that in July and August. During July, especially during the first and last 10 days of the month, deep convective activity over land in South China and offshore of Guangdong are significantly weakened. However, the deep convective activity in these regions strengthened again during the first 10 days of August, and then weakened greatly during the middle to end of September.

As shown in Figs. 3c and d, the ratio of LPCCG lightning to total CG lightning shows relatively high-frequency fluctuations over both land and sea; values of the ratio are large from June to November and low in other months. The ratio of PCG lightning to total CG lightning and of positive LPCCG lightning to LPCCG lightning over land also show trends similar to those over offshore waters. Low values of the ratios occur during May–September and high values occur in other months (except for the ratio of PCG lightning to total CG lightning over land in January, which is relatively low). Notably, the proportion of positive LPCCG lightning relative to LPCCG lightning is large during February–April, especially in February, when values reach 69.62% over land and 69.70% over offshore waters, as compared with low values in September, which decrease to 4.25% over land and 4.77% over offshore waters. In terms of seasonal comparisons, the ratios of LPCCG lightning to total CG lightning are generally higher and ratios of positive CG lightning (including PCG lightning to CG lightning and positive LPCCG lightning to LPCCG lightning) are generally lower during the rainy season than during the non-rainy season (October–March).

3.2.2. *Diurnal variation*

Distinct differences in the diurnal variations of CG lightning were observed between land and offshore waters regions, as shown in Figs. 4a and b. Over land, all types of lightning activity show a single peak at 1600–1700 LST, with vigorous lightning activity occurring from 1200 to 2100 LST. Furthermore, patterns of total CG lightning exhibit stronger fluctuations than patterns of LPCCG flashes; the peak/valley ratio for total CG lightning was 6.82, while that for LPCCG lightning was 4.66. Similarly, the peak/valley ratio for PCG lightning was 4.73, while that for positive LPCCG lightning was 3.03, also indicating that fluctuations of PCG lightning are stronger than those of positive LPCCG lightning. On the other hand, lightning activity over offshore waters exhibits two active periods, at 0300–0900 and 1400–2100 LST. The total CG lightning over offshore waters shows two peaks, with a main peak at 1600–1700 LST and a secondary peak at 0500–0600 LST. In contrast, LPCCG lightning shows a main peak at 0700–0800 LST and a secondary peak at 1800–1900 LST. Positive CG lightning activity also exhibits a primary peak in the morning and a secondary peak in the afternoon. Additionally, positive LPCCG lightning activity is relatively vigorous during the time between its two peaks (0700–0800 and 1800–1900 LST), when the total CG lightning and LPCCG lightning activity are relatively weak; thus, negative LPCCG lightning activity is substantially weaker during the two peak periods.

Diurnal variations in total CG lightning activity generally coincide with the convective activity. In a study on the climatology of deep convection over South China and adjacent seas during summer, Zheng and Cheng (2011) found that deep convection over inland areas started to strengthen at 1400 LST and peaked during 1600–1900 LST. From 2300 LST, the deep convection started to weaken, and convection was inactive during 0100–1100 LST. Over the coastal area of

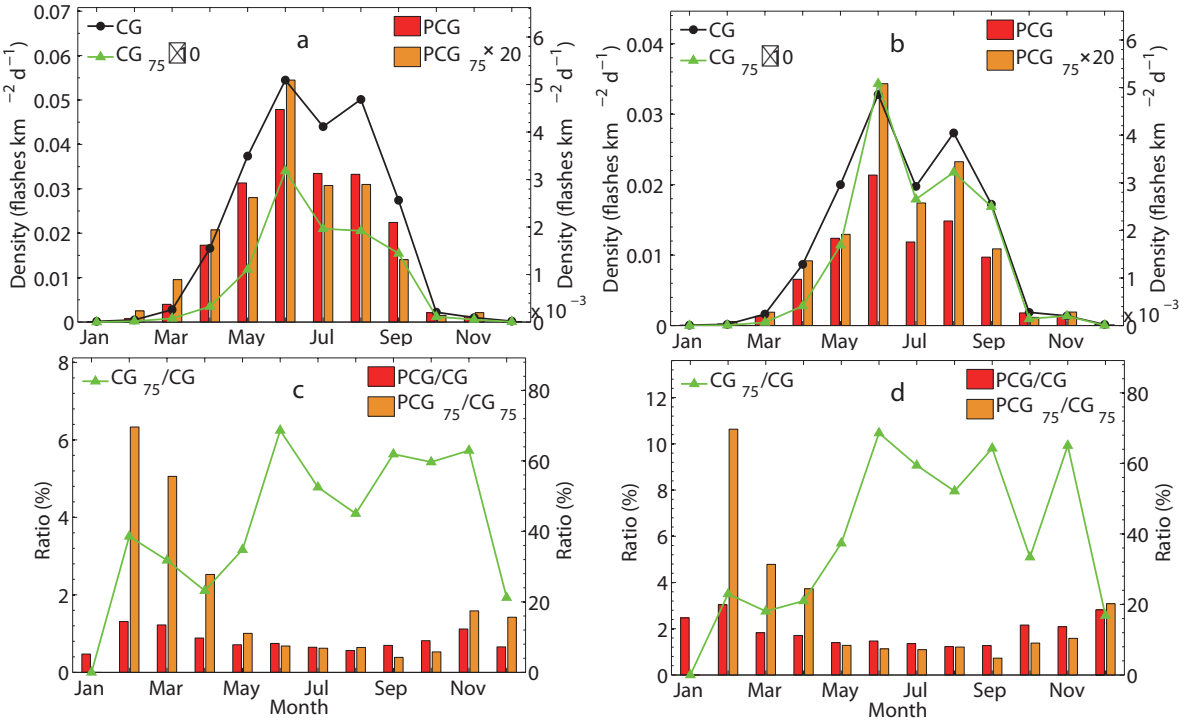

Fig. 3. Monthly distributions of CG lightning activity: (a) CG density over land; (b) CG density over offshore waters, with the *y*-axis on the left indicating CG lightning and LPCCG lightning, and the *y*-axis on the right indicating positive CG lightning (including PCG lightning and positive LPCCG lightning); (c) ratios of LPCCG to total CG lightning (left *y*-axis) and the ratios of PCG lightning to total CG lightning and positive LPCCG lightning to LPCCG lightning over land; (d) as in (c) but over offshore waters. To clearly represent and compare the variations in each graph, the values of certain types of CG lightning were multiplied by constants (shown in the legends of the figures; similarly in Fig. 4).

Guangdong, deep convection started to develop at 1200 LST, reached a peak at 1600–1800 LST, and a low at 0500 LST. In contrast, over water offshore of Guangdong, deep convection started to develop at 0200 LST, reached a peak at 1200 LST, and a low at 2300 LST. In their study on the deep convective systems over the Asian monsoon region, Wu et al. (2013) reported that continental deep convective systems were more common from noon through midnight, while oceanic deep convective systems had a dawn maximum. These characteristics indicate that deep convection is typically associated with thermal convection caused by the heating effects of solar shortwave radiation.

Diurnal variations in the ratios of different types of lightning are shown in Figs. 4c and d. The lowest ratios of LPCCG to total CG lightning occur at 1500–1600 LST over land and 1600–1700 LST over offshore waters. On the other hand, the peak in the ratio of LPCCG to total CG lightning over land occurs at 0300–0400 LST; whereas, over offshore waters, the peak occurs at 0800–0900 LST. The diurnal variations in the ratio of LPCCG to total CG lightning are reversed in comparison with that observed over land. Over offshore waters, however, the low ratios correspond to the afternoon peak in lightning activity, while the high ratios approximately correspond to the morning peak in lightning activity. Furthermore, the peak/valley ratios for the percentage of LPCCG lightning are 2.20 over offshore waters and 1.76 over land, which demonstrates that diurnal variations in the LPCCG lightning ratio are greater over offshore waters than over land.

The ratios of PCG lightning to total CG lightning and of positive LPCCG lightning to LPCCG lightning also differ between land and offshore water regions. Over land, the PCG lightning ratio generally shows diurnal variations similar to those of positive LPCCG lightning ratios, with peaks in the morning (0800–1100 LST) and valleys in the afternoon (1500–1700 LST). However, over offshore waters the ratio of PCG lightning to total CG lightning is greater in the early morning (0100–0800 LST), while the ratio of positive LPCCG lightning to total lightning is greater in the early afternoon (1300–1500 LST).

4. Relationships of lightning with precipitation and CAPE

4.1. *Lightning and precipitation*

The relationship between lightning and precipitation, which has been widely studied at climatic scales (e.g., Petersen and Rutledge, 1998; Soriano et al., 2001; Kempf and Krider, 2003; Zheng et al., 2012), is generally investigated using the rain yields per flash (RPF) parameter. Figure 5 shows the spatial distributions of rain yields per total flash (RPF_T) and rain yields per CG flash (RPF_{CG}) in the study re-

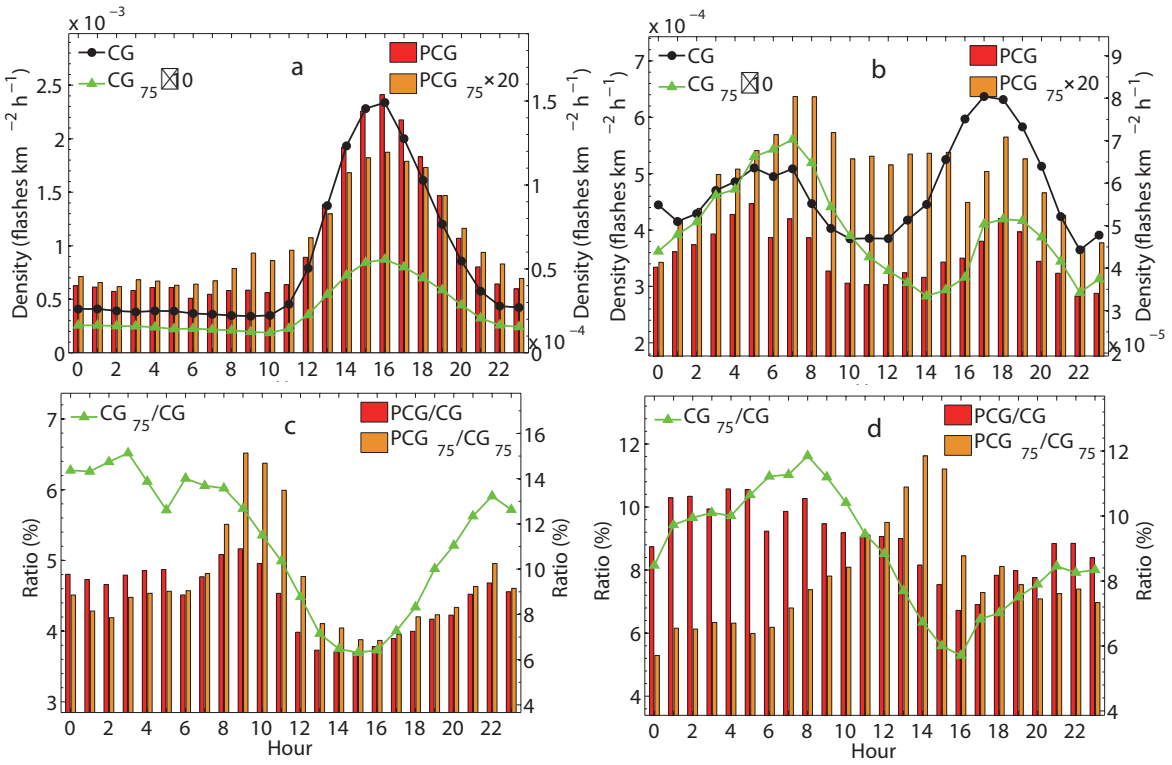

Fig. 4. Diurnal variations in CG lightning activity: (a) CG density over land; (b) CG density over offshore waters (the *y*-axis on the left indicates CG lightning and LPCCG lightning, and the *y*-axis on the right indicates PCG lightning and LPCCG lightning); (c) ratios of LPCCG to total CG lightning (left *y*-axis) and ratios of PCG lightning to CG lightning and positive LPCCG lightning to LPCCG lightning over land; (d) as in (c) but over offshore waters.

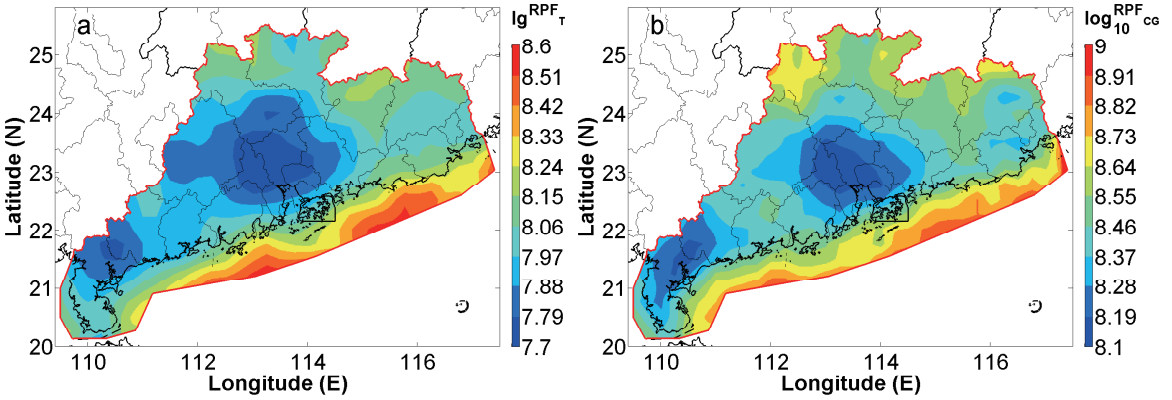

Fig. 5. Spatial distributions of (a) RPF_T and (b) RPF_{CG}. The values are given as the base-10 logarithms of the RPFs.

gion. The RPF_T is on the order of 10^7–10^8 kg per flash and the RPF_{CG} is on the order of 10^8 kg per flash; the magnitude of the latter is similar to that in the mid-continental United States, as documented by Petersen and Rutledge (1998).

A comparison of Figs. 5 and 2 shows an inverse relationship between the distribution of lightning density and that of the RPF value. Areas of low RPF occur in the PRD region and in the region to the north of Leizhou Peninsula, where strong lightning activity occurs. Areas of high RPF are located over offshore waters where the lightning density is low. A sharp gradient in the distribution of RPF values occurs along the coastline, with the slope of the gradient being opposite in direction to that of the lightning density gradient. We computed an average RPF_T value of 2.00×10^8 kg per flash and an average RPF_{CG} value of 4.72×10^8 kg per flash over offshore waters; these values are approximately 1.92 and 1.77 times greater than those over land, respectively (1.04×10^8 kg per flash and 2.66×10^8 kg per flash, respectively). Seity et al. (2001) reported a land–sea ratio of 1.8 for cumulative rainfall and 2.36 for the CG flash number over the French Atlantic coastline; therefore, the RPF value over offshore waters is approximately 1.3 times that over land in their study. As

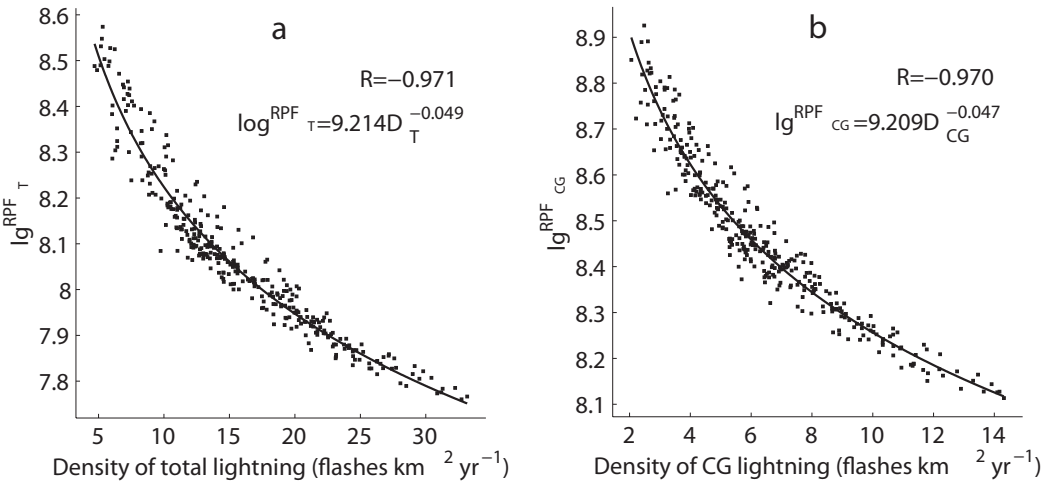

Fig. 6. Scatter plots and fitted lines that represent the correlations between the density of the total lightning and the lg (RPF_T), and between the density of the CG lightning and the lg (RPF_{CG}).

compared with Seity et al. (2001), the land–offshore contrast in the RPF value is stronger in the present study.

In previous storm-scale studies it was reported that the RPF value decreases when thunderstorms yield more lightning (e.g., López et al., 1991; Williams et al., 1992; Zipser, 1994). The climatic-scale analysis in the present study also supports this statement. To describe this inverse relationship, we evaluated various functions and found that a power function best describes the spatial correlation between lightning density (total lightning and CG lightning) and $\log_{10}$(RPF), with a correlation coefficient (R) of ~0.97 for both total lightning and CG lightning (see Fig. 6).

Because of the strong correlation between lightning frequency and convection intensity, lightning is usually regarded as a good indicator of deep convection (e.g., Zipser et al., 2006; Yuan and Qie, 2008; Xu et al., 2009; Luo et al., 2013). In addition, many studies have demonstrated a strong and significant correlation between lightning frequency and convective precipitation (e.g., Tapia et al., 1998; Soriano et al., 2001; Zheng et al., 2010). On the other hand, charging processes are closely associated with ice-phase development and ice-to-ice collisions and rebound. Therefore, a natural connection exists between lightning activity and cold-cloud precipitation. Hence, the spatial distribution of the climatic RPF value can indicate the spatial distributions of the ratio of convective precipitation to total precipitation or the contribution of cold-cloud precipitation to total precipitation. Small (large) RPF values indicate large (small) ratios of convective to total precipitation or primary (secondary) contributions of cold-cloud precipitation. According to Fig. 5, the ratio of convective to total precipitation or the contribution of cold-cloud precipitation over land were apparently larger than those over offshore waters, which is in agreement with observations that convection intensity is stronger over land than over oceans (e.g., Zipser, 1994; Zipser et al., 2006; Xu et al., 2009; Xu and Zipser, 2012; Wu et al., 2013). From Fig. 5, we further inferred that the PRD area and the region to the north of Leizhou Peninsula are characterized by more intense convection than other regions in the Guangdong area, which causes the ratio of convective to total precipitation and the contribution of cold-cloud precipitation over these regions to be larger than over other regions.

4.2. *Lightning and CAPE*

We calculated the lightning density per CAPE to investigate the impact of CAPE on lightning activity, and the sensitivity of lightning to changes in CAPE. Qie et al. (2003a) calculated a similar parameter, but examined the lightning frequency in a select region as a function of CAPE to compare the sensitivity of lightning to CAPE in different regions.

Figure 7 shows the monthly distribution of total CG lightning density per CAPE. The peak value occurred in May and the second largest value occurred in June, over both land and over offshore waters. We believe that the large values during

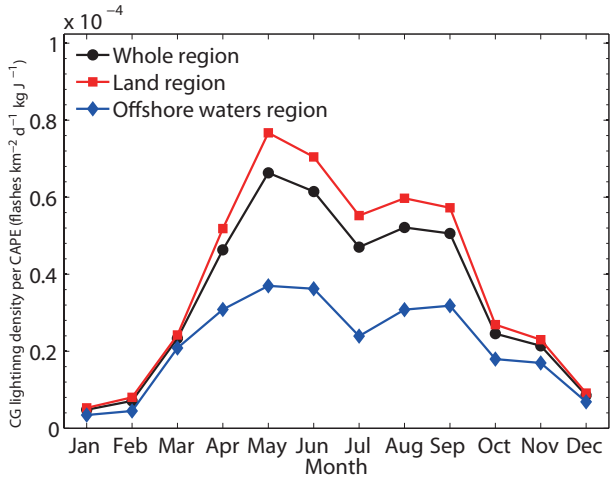

Fig. 7. Monthly distributions of the total CG lightning density per CAPE for the entire region, the land region, and the offshore waters region.

these two months are the result of monsoon systems that dominate the climate of South China from approximately mid-May to mid-June (Luo et al., 2003; Xu et al., 2009).The precipitation storms tended to be dynamically driven by large-scale weather systems (e.g., surface fronts and shear lines in the lower troposphere) during the active monsoon period, and were thermodynamically driven by local instabilities after the monsoon (Luo et al., 2003). Luo et al. (2013) further reported that CAPE values over South China increase substantially from the pre-monsoon (one continuous month before the monsoon) to the monsoon, and increase further in the post-monsoon period (one continuous month after the monsoon). Thus, high densities of lightning flashes tend to be produced by weather systems less related to transformations in CAPE during May and June, which caused the large values of total CG lightning density per CPAE during these two months. On the other hand, because monsoon weather systems are associated with circulation over a large area, including the study region, the heterogeneous spatial distribution of the contribution of monsoon weather systems to lightning could be neglected in the case of climatic analyses. Hence, the heterogeneous spatial distribution in the total CG lightning density per CAPE (Fig. 8) largely reflects the sensitivities of lightning to changes in CAPE in different areas.

Figure 8 shows that the highest sensitivity of lightning to changes in CAPE is observed in the area of the PRD, where the lightning density is greatest. In addition, lightning activity is more sensitive to CAPE over land than over offshore waters, with a sharp gradient being evident along the coast. Because of the correlation between lightning and deep convection, the large values of lightning density relative to per CAPE mean that energy transformed from CAPE can lead to more intense convection. Therefore, the distribution of values indicates the presence of stronger convection over the PRD area than other land areas, and over land than over offshore waters, which is consistent with the results estimated from the distribution of RPF values (see section 4.1). The more efficient transformation of CAPE over land is also supported by the research of Williams and Stanfill (2002), who suggested that strongly electrified continental convection is favored by a higher surface Bowen ratio, and by larger and more strongly buoyant boundary layer parcels that more efficiently transform CAPE into kinetic energy in the moist updraft stage of conditional instability. The total lightning density per CAPE values obtained in this study were 16.86×10^{-5} (unit: flashes km^{-2} d^{-1} kg J^{-1}; the same below in this paragraph) over land and 7.45×10^{-5} over offshore waters; the land/offshore waters ratio represented by the two values is 2.26. The corresponding values for CG lightning are 5.81×10^{-5} and 3.02×10^{-5} for land and offshore waters, respectively, and 1.92 for the land/offshore waters ratio.

5. Conclusions

We investigated the climatology of lightning activity and its relationships to precipitation and CAPE in South China during 2001–12, using CG lightning data observed by the GDLLS, total lightning and precipitation data obtained from the TRMM dataset, and CAPE data provided by the ERA-Interim dataset, for land areas of Guangdong Province and oceanic areas to the southeast of Guangdong Province (within ~100 km of the coastline). The main conclusions are as follows:

We identified two regions with strong lightning activity: one located in the PRD region and the other to the north of Leizhou Peninsula. A sharp gradient in lightning density was evident along the coastline. The density of LPCCG lightning is also large over the RPD, while its high density is closer to the coastline relative CG lightning The LPCCG lightning exhibits weaker land–offshore contrast compared with that of total lightning and total CG lightning. While NCG lightning features a more prominent preference for land relative to PCG lightning, the positive LPCCG lightning and negative LPCCG lightning are nearly the same in their land–offshore comparison.

The total CG lightning activity over both land and offshore waters shows peaks in June and August, although the main peak in June is more prominent over offshore waters than over land. In contrast, LPCCG lightning shows only one distinctive peak in June over land, but shows the June and August peaks over offshore waters. The ratio of LPCCG to total CG lightning is high from June to November. Regard-

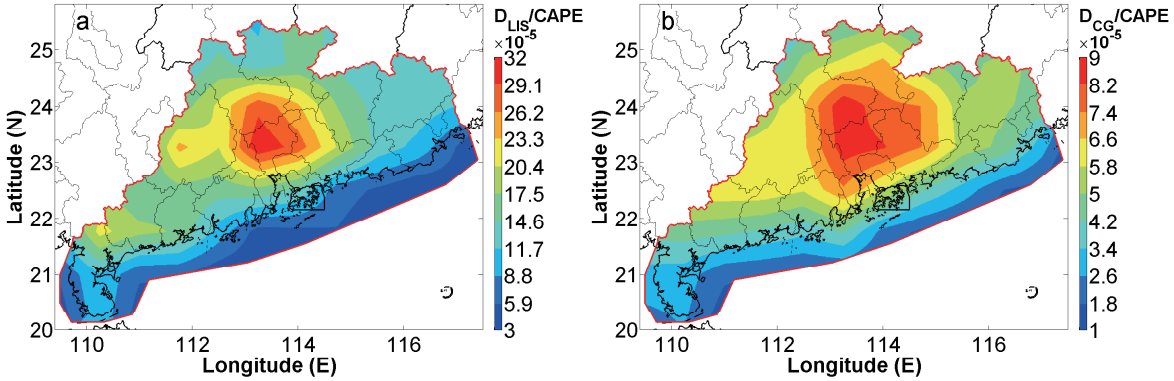

Fig. 8. Distributions of the (a) total lightning density per CAPE and (b) total CG lightning density per CAPE.

less of the total CG lightning and LPCCG lightning, the ratio of their positive components (PCG lightning and positive LPCCG lightning) is generally small during the rainy season and large during the non-rainy season. Furthermore, the ratio of positive LPCCG to total LPCCG lightning is high from February to April.

Total CG lightning and LPCCG lightning, including their positive components, both show single diurnal peaks at 1600–1700 LST over land and two diurnal peaks over offshore waters. Over land, the diurnal variations in total CG lightning are stronger than those of LPCCG flashes. Interestingly, the CG lightning over offshore waters shows a primary peak at 1600–1700 LST and a secondary peak at 0500–0600 LST, while LPCCG lightning over offshore waters shows a main peak at 0700–0800 LST and a secondary peak at 1800–1900 LST. The positive CG and LPCCG lightning components over offshore waters both show main peaks in the morning and secondary peaks in the afternoon. The ratio of LPCCG to total CG lightning peaks in the morning and decreases to a minimum in the afternoon; the peak over offshore waters lags five hours behind that over land areas. Over the land, the ratio of PCG lightning peaks in the morning (0800–1100 LST), whether for CG lightning or for LPCCG lightning; in contrast, over offshore waters, the large ratio of positive LPCCG lightning to total LPCCG lightning occurs in the early afternoon (1300–1500 LST), while that of the PCG lightning to CG lightning occurs in the early morning (0100–0800 LST).

In the study region, the spatial distribution of RPF is opposite to that of the lightning density. The average values of the RPF_T and RPF_{CG} are 2.00×10^8 kg per flash and 4.72×10^8 kg per flash, respectively, over offshore waters; these values are approximately 1.92 and 1.77 times greater, respectively, than those over land (1.04×10^8 kg per flash and 2.66×10^8 kg per flash, respectively). The spatial correlations between the densities of total lightning and CG lightning and the lg (RPF) can be described by a power function, where $R \approx 0.97$.

Lightning activity is more sensitive to CAPE over land than over offshore waters, with a sharp gradient observed along the coastline. The land/offshore waters ratio for the lightning density per CAPE is 1.92 for CG lightning and 2.26 for total lightning.

The present results demonstrate the intimate connection between lightning and convective activity, and provide further information regarding the relationship between lightning and meteorological parameters that can act as proxies for convective activity. In addition, the study highlights the apparent dependence of lightning activity on peak current and underlying surfaces, as well as the impact of underlying surfaces on the relationships between lightning and each of precipitation and CAPE. Future investigations should be conducted on the mechanisms underlying the observed climatology–lightning relationships.

Acknowledgements. This work was supported by Basic Research Fund of Chinese Academy of Meteorological Sciences (Grant No. 2013Z006 and 2014R017), National Key Basic Research Program of China (2014CB441402 and 2014CB441406), and Technology Foundation for Selected Overseas Chinese Scholar, Ministry of Personnel of China. The cloud-to-ground lightning data for this paper was provided by the State Grid Electric Power Research Institute. The ECMWF ERA-Interim data used in this study/project have been provided by ECMWF/have been obtained from the ECMWF data server at http://apps.ecmwf.int/datasets/data/interim_full_moda/. The TRMM/LIS data were processed by the TRMM Science Data and Information System (TSDIS) and the TRMM Office; they are archived and distributed by the Goddard Earth Sciences Data and Information Services Center (GES DISC). TRMM is an international project jointly sponsored by the Japan National Space Development Agency (NASDA) and the U.S. National Aeronautics and Space Administration (NASA) Office of Earth Sciences.

REFERENCES

Altaratz, O., Z. Levin, Y. Yair, and, and B. Ziv, 2003: Lightning activity over land and sea on the eastern coast of the Mediterranean. *Mon. Wea. Rev.*, **131**, 2060–2070.

Baker, M. B., H. J. Christian, and J. Latham, 1995: A computational study of the relationships linking lightning frequency and other thundercloud parameters. *Quart. J. Roy. Meteor. Soc.*, **121**, 1525–1548.

Betz, H. D., U. Schumann, and P. Laroche, 2009: *Lightning: Principles, Instruments and Applications: Review of Modern Lightning Research*. Springer, Berlin.

Boccippio, D. J., and H. J. Christian, 1999: Optical detection of lightning from space. *Proc. 11$_{\text{th}}$ International Conf. on Lightning Detection*, Guntersville, Alabama, 746–749.

Chen, L. W., Y. J. Zhang, W. T. Lu, D. Zheng, Y. Zhang, S. D. Chen, and Z. H. Huang, 2012: Performance evaluation for a lightning location system based on observations of artificially triggered lightning and natural lightning flashes. *J. Atmos. Oceanic Technol.*, **29**, 1835–1844.

Chen, S. M., Y. Du, L. M. Fan, H. M. He, and D. Z. Zhong, 2002: Evaluation of the Guang Dong lightning location system with transmission line fault data. *IEE Proceedings-Science, Measurement and Technology*, **149**(1), 9–16.

Christian, H. J., and Coauthors, 2003: Global frequency and distribution of lightning as observed from space by the Optical Transient Detector. *J. Geophys. Res.*, **108**(D1), 4005, doi: 10.1029/2002JD002347.

Coquillat, S., M.-P. Boussaton, M. Buguet, D. Lambert, J.-F. Ribaud, and A. Berthelot, 2013: Lightning ground flash patterns over Paris area between 1992 and 2003: Influence of pollution? *Atmos. Res.*, **122**, 77–92.

Cummins, K. L., M. J. Murphy, E. A. Bardo, W. L. Hiscox, R. B. Pyle, and A. E. Pifer, 1998: A combined TOA/MDF technology upgrade of the U.S. national lightning detection network. *J. Geophys. Res.*, **103**, 9035–9044.

Daniel, J. C., E. B. Buechler, and J. B. Richard, 2014: Gridded lightning climatology from TRMM-LIS and OTD: Dataset description. *Atmos. Res.*, **135-136**, 404–414.

Ding, Y. H., and Z. Y. Wang, 2008: A study of rainy seasons in China. *Meteor. Atmos. Phys.*, **100**, 121–138.

Hidayat, S., and M. Ishii, 1998: Spatial and temporal distribution of lightning activity around Java. *J. Geophys. Res.*, **103**(D12), 14 001–14 009.

Kandalgaonka, S. S., M. I. R. Tinmaker, J. R. Kulkarni, A. Nath, M. K. Kulkarni, and H. K. Trimbake, 2005: Spatio-temporal variability of lightning activity over the Indian region. *J. Geophys. Res.*, **110**(D11), D11108, doi: 10.1029/2004JD005631.

Kar, S. K., Y.-A. Liou, and K.-J. Ha, 2009: Aerosol effects on the enhancement of cloud-to-ground lightning over major urban areas of South Korea. *Atmos. Res.*, **92**, 80–87.

Kempf, N. M., and E. P. Krider, 2003: Cloud-to-ground lightning and surface rainfall during the Great Flood of 1993. *Mon. Wea. Rev.*, **131**(6), 1140–1149.

Kochtubajda, B., W. R. Burrows, and B. E. Power, 2006: Large current lightning flashes in Canada. *Proc. 2nd Conf. on Meteorological Applications of Lightning Data*, Atlanta, Georgia, USA, AMS.

Kuleshov, Y., D. Mackerras, and M. Darveniza, 2006: Spatial distribution and frequency of lightning activity and lightning flash density maps for Australia. *J. Geophys. Res.*, **111**(D19), doi: 10.1029/2005JD006982.

Kumar, P. R., and A. K. Kamra, 2010: Lightning activity variations over three islands in a tropical monsoon region. *Atmos. Res.*, **98**, 309–316.

López, R. E., R. Ortíz, W. D. Otto, and R. L. Holle, 1991: The lightning activity and precipitation yield of convective cloud systems in central Florida. *Preprints, 25th International Conf. on Radar Meteorology*, Boston, Massachusetts, USA, Amer. Meteor. Soc., 907–910.

Luo, Y. L., H. Wang, R. H. Zhang, W. M. Qian, and Z. Z. Luo, 2013: Comparison of rainfall characteristics and convective properties of monsoon precipitation systems over South China and the Yangtze and Huai River Basin. *J. Climate*, **26**, 110–132.

Lyons, W. A., M. Uliasz, and T. E. Nelson, 1998: Large peak current cloud-to-ground lightning flashes during the summer months in the Contiguous United States. *Mon. Wea. Rev.*, **126**, 2217–2233.

Ma, M., S. C. Tao, B. Y. Zhu, and W. T. Lü, 2005a: Climatological distribution of lightning density observed by satellites in China and its circumjacent regions. *Science in China Series D: Earth Sciences*, **48**(2), 219–229.

Ma, M., S. C. Tao, B. Y. Zhu, W. T. Lü, and Y. B. Tan, 2005b: Response of global lightning activity to air temperature variation. *Chinese Science Bullutin*, **50**(22), 2640–2644.

Orville, R. E., and G. R. Huffines, 2001: Cloud-to-ground lightning in the United States: NLDN results in the first decade, 1989-98. *Mon. Wea. Rev.*, **129**, 1179–1193.

Orville, R. E., G. Huffines, J. Nielsen-Gammon, R. Y. Zhang, B. Ely, S. Steiger, S. Phillips, S. Allen, and W. Read, 2001: Enhancement of cloud-to-ground lightning over Houston, Texas. *Geophys. Res. Lett.*, **28**, 2597–2600.

Orville, R. E., G. R. Huffines, W. R. Burrows, R. L. Holle, and K. L. Cummins, 2002: The North American Lightning Detection Network (NALDN)—First results: 1998-2000. *Mon. Wea. Rev.*, **130**, 2098–2109.

Pan, L. X., D. X. Liu, X. S. Qie, D. F. Wang, and R. P. Zhu, 2013: Land-sea contrast in the lightning diurnal variation as observed by the WWLLN and LIS/OTD data. *Acta Meteorologica Sinica*, **27**(4), 591–600.

Petersen, W. A., and S. A. Rutledge, 1998: On the relationship between cloud-to-ground lightning and convective rainfall. *J. Geophys. Res.*, **103**(D12), 14 025–14 040.

Pinto, O., Jr., I. R. C. A. Pinto, M. A. S. S. Gomes, I. Vitorello, A. L. Padilha, J. H. Diniz, A. M. Carvalho, and A. C. Filho, 1999a: Cloud-to-ground lightning in the southeastern Brazil in 1993: 1. Geographical distribution. *J. Geophys. Res.*, **104**, 31 369–31 380.

Pinto, I. R. C. A., O. Pinto Jr., R. M. L. Rocha, J. H. Diniz, A. M. Carvalho, and A. C. Filho, 1999b: Cloud-to-ground lightning in the southeastern Brazil in 1993: 2. Time variations and flash characteristics. *J. Geophys. Res.*, **104**, 31 381–31 387.

Pinto, O., Jr., I. R. C. A. Pinto, D. R. de Campos, and K. P. Naccarato, 2009: Climatology of large peak current cloud-to-ground lightning flashes in southeastern Brazil. *J. Geophys. Res.*, **114**, D16105, doi: 10.1029/2009JD012029.

Price, C., 1993: Global surface temperatures and the atmospheric electrical circuit. *Geophys. Res. Lett.*, **20**, 1363–1366.

Qie, X. S., R. Toumi, and Y. J. Zhou, 2003a: Lightning activity on the central Tibetan Plateau and its response to convective available potential energy. *Chinese Science Bulletin*, **48**(3), 296–299.

Qie, X. S, R. Toumi, and T. Yuan, 2003b: Lightning activities on the Tibetan Plateau as observed by the lightning imaging sensor. *J. Geophys. Res.*, **108**(D17), 4541, doi: 10.1029/2002JD 003304.

Reeve, N., and R. Toumi, 1999: Lightning activity as an indicator of climate change. *Quart. J. Roy. Meteor. Soc.*, **125**, 893–903.

Romps, D. M., J. T. Seeley, D. Vollaro, and J. Molinari, 2014: Projected increase in lightning strikes in the United States due to global warming. *Science*, **346**, 851–854.

Rudlosky, S. D., and H. E. Fuelberg, 2010: Pre-and postupgrade distributions of NLDN reported cloud-to-ground lightning characteristics in the Contiguous United States. *Mon. Wea. Rev.*, **138**, 3623–3633.

Seity, Y., S. Soula, and H. Sauvageot, 2001: Lightning and precipitation relationship in coastal thunderstorms. *J. Geophys. Res.*, **106**(D19), 22 801–22 816.

Sherwood, S. C., V. T. J. Phillips, and J. S. Wettlaufer, 2006: Small ice crystals and the climatology of lightning. *Geophys. Res. Lett.*, **33**, L05804, doi: 10.1029/2005GL025242.

Shindo, T., and S. Yokoyama, 1998: Lightning occurrence data observed with lightning location systems in Japan: 1992–1995. *IEEE Transactions on Power Delivery*, **13**, 1368–1474.

Soriano, L. R., F. de Pablo, and E. G. Diez, 2001: Relationship between convective precipitation and cloud-to-ground lightning in the Iberian Peninsula. *Mon. Wea. Rev.*, **129**(12), 2998–3003.

Steiger, S. M., and R. E. Orville, 2003: Cloud-to-ground lightning enhancement over southern Louisiana. *Geophys. Res. Lett.*, **30**(19), 1975, doi: 10.1029/2003GL017923.

Tapia, A., J. A. Smith, and M. Dixon, 1998: Estimation of convective rainfall from lightning observations. *J. Appl. Meteor.*, **37**, 1497–1509.

Wang, Y., Q. Wan, W. Meng, F. Liao, H. Tan, and R. Zhang, 2011: Long-term impacts of aerosols on precipitation and lightning over the Pearl River Delta megacity area in China. *Atmospheric Chemistry and Physics*, **11**, 12 421–12 436.

Williams, E., and S. Stanfill, 2002: The physical origin of the land-ocean contrast in lightning activity. *Comptes Rendus Physique*, **3**, 1277–1292.

Williams, E., and Coauthors, 2002: Contrasting convective regimes over the Amazon: Implications for cloud electrification. *J. Geophys. Res.*, **107**(D20), 8082, doi: 10.1029/2001JD 000380.

Williams, E. R., S. G. Geotis, N. Renno, S. A. Rutledge, E. Rasmussen, and T. Rickenbach, 1992: A radar and electrical

study of tropical "hot towers". *J. Atmos. Sci.*, **49**, 1386–1395.

Williams, E., T. Chan, and D. Boccippio, 2004: Islands as miniature continents: another look at the land-ocean lightning contrast. *J. Geophys. Res.*, **109**, D16206, doi: 10.1029/2003JD003833.

Wu, X. K., X. S. Qie, and T. Yuan, 2013: Regional distribution and diurnal variation of deep convective systems over the Asian monsoon region. *Science China Earth Sciences*, **56**(5), 843–854.

Xu, W. X., 2013: Precipitation and convective characteristics of summer deep convection over East Asia Observed by TRMM. *Mon. Wea. Rev.*, **141**, 1577–1592.

Xu, W. X., and E. J. Zipser, 2012: Properties of deep convection in tropical continental, monsoon, and oceanic rainfall regimes. *Geophys. Res. Lett.*, **39**, L07802, doi: 10.1029/2012GL051242.

Xu, W. X., E. J. Zipser, and C. T. Liu, 2009: Rainfall characteristics and convective properties of Mei-Yu precipitation systems over South China, Taiwan, and the South China Sea. Part I: TRMM observations. *Mon. Wea. Rev.*, **137**, 4261–4275.

Yi, Y. M., Z. L. Yang, and Q. L. Wan, 2006: Analysis of lightning density in Guangzhou City. *Resources Science*, **28**(1), 151–156. (in Chinese)

Yuan, T., and X. S. Qie, 2008: Study on lightning activity and precipitation characteristics before and after the onset of the South China Sea summer monsoon. *J. Geophys. Res.*, **113**, D14101, doi: 10.1029/2007JD009382.

Zhang, M. F., X. S. Liu, Y. J. Zhang, M L. Fan, D. Z. Zhong, and L. C. Zhou, 2000: Preliminary study on climatological distributions of lightning flash in Guangdong. *Journal of Tropical Meteorology*, **16**(1), 46–53. (in Chinese)

Zhang, W. J., Q. Meng, M. Ma, and Y. J. Zhang, 2011: Lightning casualties and damages in China from 1997 to 2009. *Natural Hazards*, **57**, 465–476.

Zheng, D., J. R. Dan, Y. J. Zhang, C. Wu, and C. J. Zeng, 2012: Regional differences of relationship between cloud-to-ground lightning and precipitation in China. *Journal of Tropical Meteorology*, **28**(4), 569–576. (in Chinese)

Zheng, D., Y. J. Zhang, Q. Meng, and W. T. Lü, 2010: Relationship between lightning activities and surface precipitation in thunderstorm weather in Beijing. *Journal of Applied Meteorological Science*, **21**(3), 287–297. (in Chinese)

Zheng, Y. G., and J. Cheng, 2011: A climatology of deep convection over south China and adjacent seas during summer. *Journal of Tropical Meteorology*, **27**(4), 495–508. (in Chinese)

Zipser, E. J., 1994: Deep cumulonimbus cloud systems in the tropics with and without lightning. *Mon. Wea. Rev.*, **122**, 1837–1851.

Zipser, E. J., C. T. Liu, D. J. Cecil, S. W. Nesbitt, and D. P. Yorty, 2006: Where are the most intense thunderstorms on Earth? *Bull. Amer. Meteor. Soc.*, **87**, 1057–1071.